



ENHANCING THE PHOTOCURRENT BY TiO₂ NANOFIBERS IN PbS QUANTUM DOT – SENSITIZED SOLAR CELLS

T. Jaseetharan^{1,2}, W.I. Sandamali^{2,3*}, G.K.R. Senadeera^{2,3}, V.P.S. Perera³, J.C.N. Rajendra³, N. Karthikeyan³, Lahiru A. Wijenayaka⁴, M.A.K.L. Dissanayake²

¹Department of Physical Sciences, South Eastern University of Sri Lanka, Sri Lanka

²National Institute of Fundamental Studies, Sri Lanka

³Department of Physics, The Open University of Sri Lanka, Sri Lanka

⁴Department of Chemistry, The Open University of Sri Lanka, Sri Lanka

INTRODUCTION

Quantum dot-sensitized solar cells (QDSSCs) have gained more attention recently in the area of solar power conversion systems due to their low production cost and the excellent properties of quantum dots such as ability of multiple exciton generation (MEG), tuneable energy gap due to the quantum confinement effect and high molar extinction coefficients. The working principle and structure of QDSSC is similar to the dye-sensitized solar cell. Only difference between these solar cells is the sensitizer. In dye-sensitized solar cells, organic or metal organic dyes are used as sensitizers while in the case of QDSSC, the dyes are replaced by inorganic semiconductor quantum dots.

PbS quantum dot is an IV-VI type semiconductor with a bulk bandgap of 0.41 eV and a large exciton Bohr radius of 18 nm. It has high photosensitivity in the near-infrared region and due to the quantum confinement effect, the energy gap can be tuned for the absorption of visible to infrared photons (Moreels et al., 2009). PbS quantum dots have attracted work in various optoelectronic devices including infrared detectors (Clifford et al., 2007; Heves & Gurbuz, 2012; Mi et al., 2017) and quantum dot-sensitized solar cells (Yoon et al., 2013; Zhao et al., 2010). Performance of QDSSCs can be enhanced by increasing the light absorption by scattering effect. Light scattering can be improved by introducing different layers having different surface morphological structures to the photoanodes. For example, Wan *et al.* reported TiO₂ nanorod array based QDSSC with an efficiency of 3.14% (Wan et al., 2016). The surfaces of the nanorods were etched and nano caves were formed. These structures enhance the surface area of the photoanode for CdS quantum dot formation and enhance the diffused reflectance ability of the photoanode.

In the present study, TiO₂ nanoparticle photoanode based PbS QDSSCs have been fabricated with suitable SILAR cycles. Number of SILAR cycles for the best solar cell has been optimized. In order to enhance the performance of the solar cells by enhanced light absorption by scattering, the same thickness TiO₂ nanofiber electrodes have been fabricated and sensitized with PbS quantum dots.

METHODOLOGY

Preparation of TiO₂ Nanoparticle (NP) electrodes

A pinhole free compact layer (CL) of TiO₂ was first deposited on a pre-cleaned FTO glass substrate by the following method. 1 ml of titanium (IV) isopropoxide, 1 ml of propan-1-ol, 1 ml of glacial acetic acid and 1 drop of con. HNO₃ was added to 8 ml of ethanol and the mixture was mixed well. This solution was then spin coated on the conducting side of the FTO glass substrate at 3000 rpm for 1 minute. Substrate was sintered at 450 °C for 45 minutes. The above substrate with a compact layer was then covered with a paste prepared with P90 TiO₂ as follows. 0.25 g of TiO₂ P90 powder was ground well for 15 minutes with 1 ml of 0.1 M HNO₃. The paste was spin coated on the TiO₂ compact layer at 3000 rpm for 1 minute and sintered at 450 °C for 45 minutes. For preparation of TiO₂ P25 paste, 0.25 g of TiO₂ powder and 1 ml of 0.1 M HNO₃ were ground using mortar and pestle. Then, 0.02 g of Triton X-100 and 0.05 g of Poly ethylene glycol 1000 were used as the binder and the mixture was ground until it became a creamy paste (Kumari et al., 2017). This TiO₂ P25 paste was spin coated on TiO₂ CL/TiO₂ P90 layer at 1000 rpm for 1 minute. Then the electrode was sintered at 450 °C for 45 minutes.



Preparation of TiO₂ Nanofiber (NF) electrodes

On top of the TiO₂ CL/TiO₂ P90 electrode a TiO₂ nanofiber layer was deposited. Initially, 9.5 ml of N,N-dimethylformamide and 0.5 ml of glacial acetic acid were thoroughly mixed. Subsequently, 1.5 ml of titanium (IV) isopropoxide was added to the mixture which was subjected to magnetic stirring for 20 minutes. Finally, 0.75 g of poly (vinyl acetate) was added to the mixture and magnetically stirred for 4 hours. A TiO₂ nanofiber (NF) layer was deposited for 20 minutes with a solution flow rate of 2 ml h⁻¹ on the FTO/TiO₂ CL/ TiO₂ P90 layer by electrospinning (NaBond Electrospinner, NaBond Technologies, Hong Kong). During the electrospinning, the voltage difference and the distance between the spinneret and photoanode were kept at 15 kV and 6.5 cm respectively (Dissanayake et al., 2016).

Deposition of quantum dots

PbS quantum dots were deposited on TiO₂ electrodes by successive ionic layer adsorption and reaction (SILAR) method. Aqueous solutions of 0.1 M Pb(NO₃)₂ and 0.1 M Na₂S were used as cationic precursor solution and anionic precursor solution respectively. In this method, electrodes are immersed alternatively into cationic and anionic precursor solutions. Between immersing processes, the electrode was rinsed in deionized water and dried.

Preparation of polysulfide electrolyte

Polysulfide electrolyte was prepared by dissolving 2 M Na₂S and 2 M S in a mixture of water and methanol in the ratio of 3:7 (v/v). The mixture was subjected to magnetic stirring at room temperature until all the sulfur was dissolved.

Preparation of Cu₂S counter electrode

A cleaned brass plate was immersed in conc. HCl at 80 °C for 10 minutes. A scotch tape mask with an appropriate area was applied on the surface of the treated brass plate. Synthesized polysulfide electrolyte was applied to the unmasked area which became black in colour due to the formation of Cu₂S. This electrode was used as the counter electrode of the QDSSCs.

Cell assembly and current-voltage characterization

An appropriate amount of polysulfide electrolyte was applied on the unmasked area of the Cu₂S counter electrode. TiO₂ photoanode was placed on the electrolyte so that the active sides of both electrodes were facing each other with the electrolyte in between them and held together using steel clips. Current-voltage measurements of each QDSSCs were done under the illumination of 100 mW cm⁻² with AM 1.5 spectral filter using a computer controlled multi-meter (Keithley 2000 model) coupled with potentiostat/galvanostat unit (HA-301). The active area of the QDSSC was 0.12 cm².

Optical absorption measurements

Optical absorption spectra of PbS quantum dot-sensitized TiO₂ nanoparticle electrodes and TiO₂ nanofiber electrode were obtained using Shimadzu 2450 spectrophotometer in the wavelength range between 350 nm to 1100 nm.

Surface morphology of the electrodes

SEM images of the TiO₂ nanoparticle layer and TiO₂ nanofiber layer were obtained by using the ZEISS EVO scanning electron microscope.

RESULTS AND DISCUSSION

Figure 1 shows the optical absorption spectra of bare TiO₂ electrodes and PbS quantum dot-sensitized TiO₂ electrodes with different SILAR cycles. Absorption of the photoanode increases with the number of SILAR cycles. Each spectrum corresponding to the TiO₂/PbS electrodes exhibits a broad absorption in the visible to near-infrared region. However, a suitable number of SILAR cycles for the solar cell application was identified by the current-voltage characteristics of the fabricated PbS QDSSCs. A peak



corresponding to the lowest energy absorption is known as the first excitonic absorption peak (Mcdonald et al., 2005).

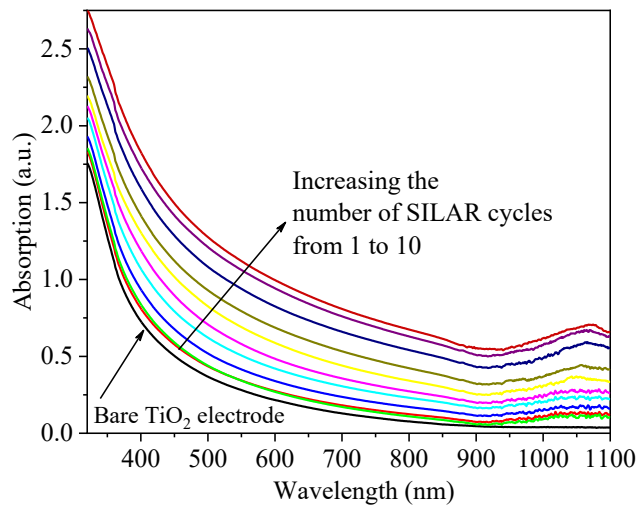


Figure 1: Absorption spectra of TiO₂ NP electrode and PbS quantum dot-sensitized TiO₂ NP electrodes.

Photoanodes show the first excitonic absorption peaks at 1021, 1025, 1036, 1039, 1042, 1050, 1057, 1063, 1068 and 1083 nm corresponding to the number of SILAR cycles from 1 to 10 respectively. Increasing the wavelength corresponding to the absorption maximum clearly reveals that the size of the quantum dots increases with the number of SILAR cycles (Ahmed et al., 2012).

Figure 2 shows the variation of efficiency with the number of SILAR cycles. The efficiency of the PbS QDSSCs gradually increases with the number of SILAR cycles and shows a maximum efficiency corresponding to 6 SILAR cycles. The size and number of quantum dots increase with the number of SILAR cycles. When the number of SILAR cycles increases beyond 6, the efficiency of the QDSSCs decreases. The increase in the number of SILAR cycles leads to an increase in the size of the quantum dots which affects the average distance between the quantum dots and TiO₂ nanostructure. Furthermore, the number of quantum dots increases with the number of SILAR cycles, which causes aggregation and the performance of the solar cell is reduced as described by Guijarro *et al.* (Guijarro et al., 2010). Kern *et al.* reported that aggregation of quantum dots can affect the average electronic coupling and increase the average distance between the TiO₂ and quantum dots (Kern & Watson, 2014). Due to this nature, charge transfer between quantum dots and TiO₂ is decreased and the performance of the QDSSC decreases.

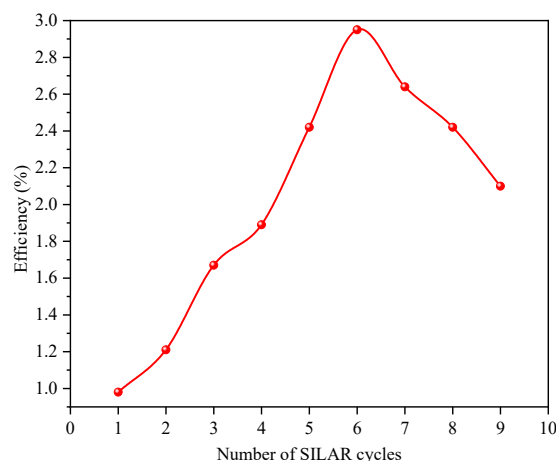




Figure 2: Variation of efficiency of PbS QDSSCs with number of SILAR cycles where TiO₂ NP electrode is used

Figure 3 illustrates the aggregation and increasing the size of PbS quantum dots during the SILAR process with a large number of cycles.

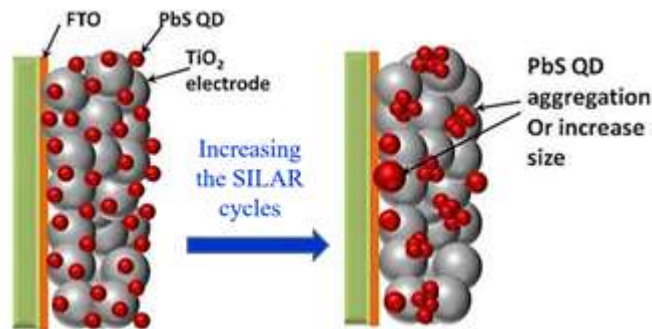


Figure 3: Schematic diagram of aggregation of quantum dots on TiO₂ electrode.

Figure 4 (a) and (b) show the top view of the TiO₂ nanoparticle and nanofiber layers respectively. The size of the nanofibers with the average diameter appears to be between 30 and 80 nm. This nanostructured layer enhances the light absorption of the photoanode by multiple light scattering.

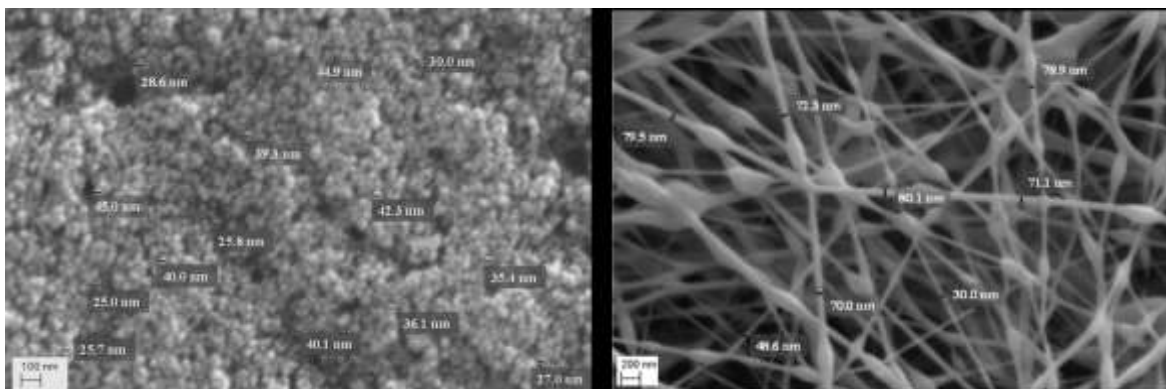


Figure 4: SEM images of (a) TiO₂ nanoparticle electrode and (b) TiO₂ nanofiber electrode.

Figure 5 shows the absorption spectra of the PbS quantum dot incorporated TiO₂ nanoparticle and nanofiber electrodes. The nanofiber photoanode shows better efficiency due to the scattering.

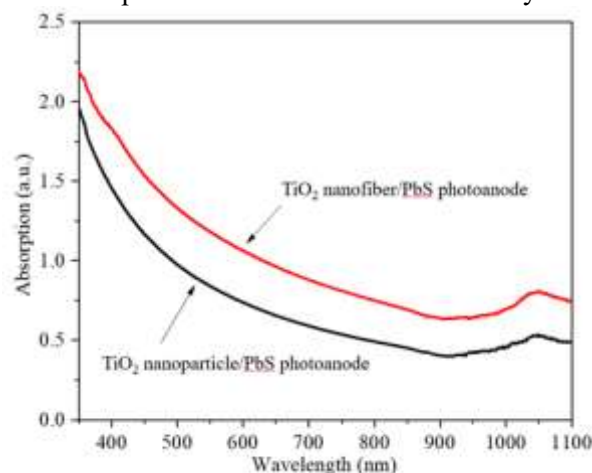




Figure 5: Absorption spectra of PbS quantum dot incorporated TiO₂ nanoparticle and nanofiber photoanodes

Figure 6 shows the current-voltage characteristics of PbS QDSSCs fabricated with TiO₂ nanoparticle layer photoanode and TiO₂ nanofiber photoanode under the illumination of 100 mW cm⁻² with AM 1.5 spectral filter. TiO₂ NF photoanode shows better photovoltaic performance than the TiO₂ NP photoanode. Photovoltaic parameters corresponding to the photoanodes are listed in table 1.

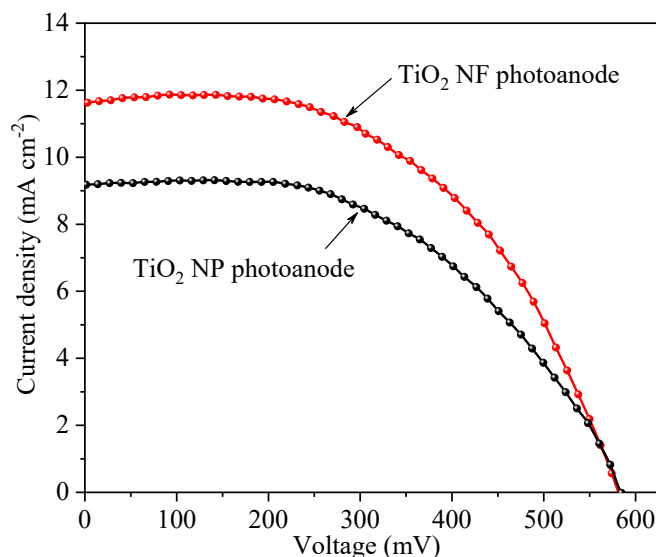


Figure 6: Current-voltage characterization of PbS QDSSCs under the illumination of 100 mW cm⁻² with AM 1.5 spectral filter

Table 1: Photovoltaic parameters of PbS QDSSCs

TiO ₂ Photoanode	J_{SC} (mA cm ⁻²)	V_{OC} (mV)	FF (%)	Efficiency (%)
Nanoparticle (NP)	9.22	582.4	55.0	2.95
Nanofiber (NF)	11.64	580.6	58.0	3.92

QDSSC with TiO₂ NF photoanode shows an efficiency of 3.92% with a higher short-circuit current density of 11.64 mA cm⁻². The corresponding QDSSC made with TiO₂ nanoparticles (NP) only shows an efficiency of 2.95%. The enhancement in overall power conversion efficiency of the PbS QDSSC with nanofiber photoanode relative to the nanoparticle photoanode is about 33%. It can be concluded that the enhancement in short-circuit current density is evidently due to the increased light absorption by multiple light scattering.

CONCLUSIONS/RECOMMENDATIONS

TiO₂ nanoparticle electrode-based QDSSCs shows an efficiency of 2.95% and a short-circuit current density of 9.22 mA cm⁻² while QDSSC with TiO₂ nanofiber photoanode shows an efficiency of 3.92% with a higher short-circuit current density of 11.64 mA cm⁻². It can be seen that the enhancement in short-circuit current is evidently due to the increased light absorption by multiple light scattering and effective electron injection.

REFERENCES

Ahmed, R., Will, G., Bell, J., & Wang, H. (2012). Size-dependent photodegradation of CdS particles deposited onto TiO₂ mesoporous films by SILAR method. *Journal of Nanoparticle Research*, 14(9). <https://doi.org/10.1007/s11051-012-1140-x>



- Clifford, J. P., Johnston, K. W., Levina, L., & Sargent, E. H. (2007). Schottky barriers to colloidal quantum dot films. *Applied Physics Letters*, *91*(25). <https://doi.org/10.1063/1.2823582>
- Dissanayake, M. A. K. L., Divarathna, H. K. D. W. M. N., Dissanayake, C. B., Senadeera, G. K. R., Ekanayake, P. M. P. C., & Thotawattage, C. A. (2016). An innovative TiO₂ nanoparticle/nanofibre/nanoparticle, three layer composite photoanode for efficiency enhancement in dye-sensitized solar cells. *Journal of Photochemistry and Photobiology A: Chemistry*, *322–323*, 110–118. <https://doi.org/10.1016/j.jphotochem.2016.02.017>
- Guijarro, N., Lana-Villarreal, T., Shen, Q., Toyoda, T., & Gómez, R. (2010). Sensitization of titanium dioxide photoanodes with cadmium selenide quantum dots prepared by SILAR: Photoelectrochemical and carrier dynamics studies. *Journal of Physical Chemistry C*, *114*(50), 21928–21937. <https://doi.org/10.1021/jp105890x>
- Heves, E., & Gurbuz, Y. (2012). PbS colloidal quantum dot photodiodes for SWIR detection. *Procedia Engineering*, *47*, 1426–1429. <https://doi.org/10.1016/j.proeng.2012.09.425>
- Kern, M. E., & Watson, D. F. (2014). Linker-assisted attachment of cdse quantum dots to TiO₂: Time- and concentration-dependent adsorption, agglomeration, and sensitized photocurrent. *Langmuir*, *30*(44), 13293–13300. <https://doi.org/10.1021/la503211k>
- Kumari, J. M. K. W., Senadeera, G. K. R., Dissanayake, M. A. K. L., & Thotawattage, C. A. (2017). Dependence of photovoltaic parameters on the size of cations adsorbed by TiO₂ photoanode in dye-sensitized solar cells. *Ionics*, *23*(10), 2895–2900. <https://doi.org/10.1007/s11581-017-1995-z>
- Mcdonald, S. A., Konstantatos, G., Zhang, S., Cyr, P. W., Klem, E. J. D., Levina, L., & Sargent, E. H. (2005). Solution-processed PbS quantum dot infrared photodetectors and photovoltaics. *Nature Materials*, *4*(2), 138–142. <https://doi.org/10.1038/nmat1299>
- Mi, L., Wang, H., Zhang, Y., Yao, X., & Chang, Y. (n.d.). *application High performance visible – near-infrared PbS- quantum-dots / indium Schottky diodes for photodetectors.*
- Moreels, I., Lambert, K., Smeets, D., & De Muynck, D. (2009). Size-Dependent Optical Properties of Colloidal PbS Quantum Dots - ACS Nano (ACS Publications). *Acs Nano*, *3*(10), 3023–3030. <http://pubs.acs.org/doi/abs/10.1021/nn900863a>
- Wan, J., Liu, R., Tong, Y., Chen, S., Hu, Y., Wang, B., Xu, Y., & Wang, H. (2016). Hydrothermal etching treatment to rutile TiO₂ nanorod arrays for improving the efficiency of CdS-sensitized TiO₂ solar cells. *Nanoscale Research Letters*, *11*(1), 1–9. <https://doi.org/10.1186/s11671-016-1236-9>
- Yoon, W., Boercker, J. E., Lumb, M. P., Placencia, D., Foos, E. E., & Tischler, J. G. (2013). Enhanced open-circuit voltage of PbS nanocrystal quantum dot solar cells. *Scientific Reports*, *3*, 1–7. <https://doi.org/10.1038/srep02225>
- Zhao, N., Osedach, T. P., Chang, L., Geyer, S. M., Wanger, D., Binda, M. T., Arango, A. C., Bawendi, M. G., & Bulovic, V. (2010). *Colloidal PbS Quantum Dot Solar Cells with High Fill Factor.* *4*(7), 3743–3752.

ACKNOWLEDGMENTS

This research was supported by the Accelerating Higher Education Expansion and Development (AHEAD) Operation (DOR 09) of the Ministry of Higher Education funded by the World Bank.